Functionalized zinc porphyrin as light harvester in dye sensitized solar cells

L GIRIBABU,[a,*] CH VIJAY KUMAR,[a] M RAGHAVENDER,[a] K SOMAIAH,[a] P YELLA REDDY[a] and P VENKATESWARA RAO[b]

[a]Nanomaterials Laboratory, Inorganic and Physical Chemistry Division,
Indian Institute of Chemical Technology, Hyderabad 500 007
[b]Department of Chemistry, Nizam College (Osmania University), Hyderabad 500 001
e-mail: giribabu@iict.res.in

Abstract. A new photosensitizer having two rhodanine acetic acid groups at *meso*-positions of a zinc porphyrin [*meso*-Rhod-Zn-Rhod] has been synthesized and characterized by UV-Visible, ^{1}H NMR, MALDI-MS, fluorescence spectroscopies and cyclic voltammetry. The new photosensitizer was tested in dye-sensitized solar cells with three different liquid redox electrolytes and compared its efficiency (η) with dyad. Both dyad and triad were also tested in DSSC using a polymer gel redox electrolyte and observed low efficiency because of small short circuiting current i.e. I_{Sc} though the IPCE is significantly high. The probable reason for the low efficiency small I_{Sc} has been attributed to the internal resistance of the cell.

Keywords. Porphyrins; triad; solar cells; gel electrolyte; quasi-solid state.

1. Introduction

Nanocrystalline dye-sensitized solar cells (DSSC's) have attracted significant attention for the last one and half decade as environmentally pleasant and low cost alternatives to conventional solid-state photo-voltaic devices.[1–4] The most successful charge transfer sensitizer employed so far in such cells, *cis*-dithio-cyanatobis-(2,2′-bipyridyl-4,4′-dicarboxylate) ruthenium(II) (together with its various protonated forms), its modified forms and trithiocyanato 4,4′4″-tricaboxy-2,2′ : 6′,2″-terpyridine ruthenium(II) (the black dye), yields conversion efficiencies of up to 10–11% under air mass (AM) 1·5 solar conditions with liquid redox electrolyte.[5–7] Though these cells show high conversion efficiency, there remain some significant limitations, in particular the liquid redox electrolyte which leads to several technical disadvantages: solvent evaporation and degradation limit the long-term durability, low temperature may effect the solubility of salts, high temperatures enhance the volatility of the solvent, and diffusion sometimes limit the kinetics under high light intensities. Thus there are practical advantages for replacing the liq-

uid electrolyte system with polymer gel materials, a quasi-solid-state DSSC. Another important requisite to improve the efficiency of DSSC, is the absorption of dye in IR and near-IR response of the solar emission. Hence, the important requirement for highly efficient DSSC operation is that the sensitizer should be panchromatic, that is, absorbing visible light of all colours as well as durability.

Besides polypyridyl complexes, a variety of alternative sensitizers have been explored in dye-sensitized solar cells, in particular metal-free sensitizers (synthetic organic dyes), the porphyrins and phthalocyanine class of dyes.[8–11] However, organic dyes based DSSCs are not useful for rooftop applications, as these organic molecules are not exceedingly long-lasting. In contrast, given their primary role in natural photosynthesis, the use of porphyrins as light harvesters on semiconductor is particularly attractive over recent years due to the fact of better understanding of the role of porphyrin molecules in natural photosynthetic process.[12–14] Porphyrins exhibit long-lived (> 1 ns) singlet excited state and only weak singlet/triplet mixing. They have an appropriate LUMO level that resides above the conduction band of the TiO_2 and HOMO level that lies below the redox couple in the electrolyte solution, required
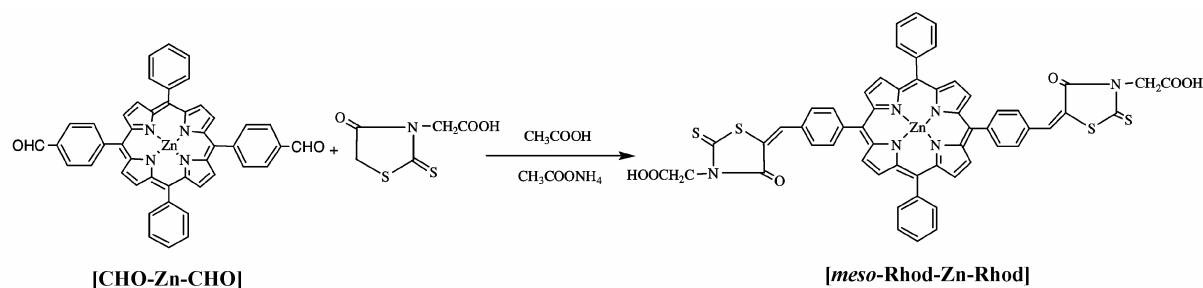
Scheme 1.

for charge separation at SC/dye/electrolyte surface. Various porphyrins have been used for the photosensitization of wide-band-gap semiconductors (SCs) like NiO, ZnO and TiO_2, the most common being the free-base and zinc derivatives of the *meso*-benzoic acid substituted porphyrin. In contrast, other workers have tested pyrrole-β substituted porphyrins as photosensitizers for nanocrystalline TiO_2 semiconductor. It is observed that the zinc porphyrin with extended π-conjugated acrylic acid derivative, which has shown the efficiency as high as of 5.2%.[15,16]

Recently, we have reported porphyrin-rhodanine acetic acid dyads based DSSC, having rhodanine moiety either at *meso*- or pyrrole-β position of a freebase/metallo-porphyrin.[9] It was observed that zinc porphyrin having rhodanine moiety at *meso*-position, {4-oxo-2-thioxo-5-[4-(10, 15, 20-triphenyl-porphyrinato zinc(II)-5-yl)-benzylidene}-thiazolidin-3yl}-acetic acid [*meso*-Zn-Rhod], is more efficient than its pyrrole-β substituted dyad, [4-oxo-5-(5,10,15,20-tetraphenyl-porphyrinato zinc(II)-2-ylmethylene)-2-thioxo-thiazolidin-3-yl]-acetic acid [β-Zn-Rhod]. In the present investigation, we report a DSSC having a photosensitizer with two rhodanine moieties at *meso*-positions of zinc porphyrin i.e. [[5-(4-{15-[4-(3-carboxymethyl-4-oxo-2-thioxo-thiazolidin-5-ylidene-methyl)-phenyl]-10,20-diphenyl porphyrinato zinc(II)-5yl}-benzylidene)-4-oxo-2-thioxo-thiazolidin-3-yl]-acetic acid] i.e. [*meso*-Rhod-Zn-Rhod] triad system and tested its efficiency in DSSC. The proposed structure of the sensitizer was shown in scheme 1. This new sensitizer was tested in DSSC with liquid as well as polymer gel electrolyte and compared its performance with the dyad [*meso*-Zn-Rhod].

2. Experimental

The chemicals and solvents utilized in this study were purchased from either Aldrich Chemical Co. (USA) or BDH (Mumbai, India). The solvents uti-

lized for spectroscopic and electrochemical experiments were further purified using the standard procedures.[17] The compounds 5,10,15,20-tetraphenyl porphyrin (H_2TPP), 5,10,15,20-tetraphenyl porphyrinato zinc(II) (ZnTPP) and 5,15-*bis*-(4-cyano phenyl)-10,20-bisphenyl porphyrinato zinc(II) [CN-Zn-CN] were synthesized according to the procedure as reported in the literature.[18]

2.1 *Synthesis*

2.1a *5,15-bis-(4-formyl phenyl)-10,20-bisphenyl porphyrinato zinc(II) [CHO-Zn-CHO]:* 5,15-*bis*-(4-cyano phenyl)-10,20-bisphenyl porphyrinato zinc(II) (100 mg, 0·14 mmol) was dissolved in 50 ml of dry dichloromethane. To this reaction mixture DIBAL-H (1·0 M in hexane, 1·0 ml) was added drop-wise at 0°C. Then the reaction mixture was brought to room temperature and stirred for 4 h. To this 20 ml of ammonium hydroxide was added and stirring was continued another 15 min. The solvent was removed under reduced pressure. The obtained solid material was subjected to silica gel column chromatography and eluted with chloroform. The solvent front running band was collected and recrystallized. UV-Visible (in ethanol, λ_{max}, logε): 421 (4·79); 565 (3·85); 608 (3·57). ^{1}H NMR (CDCl$_3$, δ, ppm): 10·32 (*s*, 2H); 8·92 (*m*, 8H); 8·45 (*d*, 4H, $J = 7·8$ Hz); 8·35 (*d*, 4H, $J = 7·8$ Hz); 8·20 (*m*, 4H), 7·72 (*m*, 6H), 7·55 (*d*, 2H, $J = 6·2$ Hz). MALDI-MS: $C_{46}H_{28}N_4O_2Zn$ [734]: M$^+$ 734 (75%). Anal. Calcd. for $C_{46}H_{28}N_4O_2Zn$, % (734·13): C, 75·26; H, 3·84; N, 7·63. Found C, 75·10; H, 3·80; N, 7·60.

2.1b *[meso-Rhod-Zn-Rhod]:* This compound was synthesized according to the reported procedure in the literature.[9] 5,10-*bis*-(4-formyl phenyl)-15,20-bisphenyl porphyrinato zinc(II) (100 mg, 0·11 mmol) and rhodanine acetic acid (192 mg, 1·0 mmol), ammonium acetate (12 mg, 0·16 mmol) was dissolved

in 25 ml of acetic acid. The resulting reaction mixture was refluxed for 24 h and then cooled to the room temperature. The reaction mixture was poured into water and the compound was precipitated. The precipitate was filtered and dried. The obtained compound was subjected to silica gel column chromatography and eluted with $CHCl_3/CH_3OH$ (7 : 3%). The first band was the unreacted zinc *meso-bis*-formyl porphyrin. The second dark brown colour band was the desired compound. The solvent was removed under reduced pressure and recrystallized from methanol. The compound was characterized by UV-Visible, ^{1}H NMR, MALDI-MS and CHN analysis. UV-Visible (in ethanol, λ_{max}, $\log \varepsilon$): 436 (4·73); 561 (3·73); 604 (3·87). ^{1}H NMR (DMSO-d_6, δ, ppm): 8.88 (*m*, 8H); 8·38 (*d*, 4H, $J = 8·2$ Hz); 8·20 (*d*, 4H, $J = 6·8$ Hz); 8·15 (*s*, 2H); 7·90 (*d*, 4H, $J = 8·2$ Hz), 7·72 (*m*, 4H), 7·55 (*d*, 2H, $J = 6·2$ Hz) and 4·80 (*b*, 2H). MALDI-MS: $C_{56}H_{34}N_6O_6S_4Zn$ [1078]: M^+ 1079 (40%). Anal. Calcd. for $C_{56}H_{34}N_6O_6S_4Zn$, % (1078·07): C, 62·25; H, 3·17; N, 7·78. Found C, 62·30; H, 3·15; N, 7·60.

2.2 *Methods*

The UV-Visible spectra were recorded with a Shimadzu model 170 spectrophotometer for 1×10^{-6} M (porphyrin Soret band) and 5×10^{-5} M (porphyrin Q-bands) solutions. Steady state fluorescence spectra were recorded using a Spex model Fluoromax-3 spectrofluoremeter for solutions having optical density at the wavelength of excitation (λ_{ex}) $\approx 0·11$. The fluorescence quantum yields (ϕ) were estimated by integrating the fluorescence bands and by using 5,10,15,20-tetraphenyl porphyrinato zinc(II) (ZnTPP) ($\phi = 0·036$ in CH_2Cl_2) as the standard.[19] MALDI-MS spectra were recorded on a TO-4X KOMPACT SEQ, KARTOS, UK, mass spectrometer. Major fragmentations are given as percentages relative to the base peak intensity. ^{1}H NMR spectra were obtained at 300 MHz using a Brucker 300 Avance NMR spectrometer running X-WIN NMR software. The chemical shifts are relative to tetramethylsilane (TMS). The Fourier transform IR (FTIR) spectra were measured using a Thermo Nicolet Nexus 670 spectrometer.

Cyclic- and differential pulse voltammetric measurements were performed on a PC-controlled CH instruments model CHI 620C electrochemical analyzer. Cyclic voltammetric experiments were performed on 1 mM porphyrin triad solution in methanol at a scan rate of 100 mV/s using 0·1 M tetrabutyl ammonium-hexafluorophosphate ($TBAPF_6$) as supporting electrolyte. The working electrode is glassy carbon, standard calomel electrode (SCE) is reference electrode and platinum wire is an auxillary electrode. After a cyclic voltammogram (CV) had been recorded, ferrocene was added, and a second voltammogram was measured.

2.3 *TiO₂ electrode preparation and cell fabrication*

TiO_2 photoelectrode (area: ca. 0·74 cm^2) was prepared by a similar method as reported in the literature.[20,21] TiO_2 anatase nanoparticles of 19 nm were procured from Solaronix. Nanocrystalline TiO_2 films of 6 μm were deposited onto transparent conducting glass (the glass had been coated with a fluorine-doped stannic oxide layer (FTO); sheet resistance 8–10 Ω/square) by screen-printing technique. Nanocrystalline TiO_2 films were heated to 450°C in an oxygen atmosphere and calcinated for 45 min. The dye was dissolved in ethanol at a concentration of $0·05 \times 10^{-3}$ M. The TiO_2 films were soaked in the dye solution and then kept at room temperature for 16 h so that the dye was adsorbed onto TiO_2 films. The photoelectrode was dipped into the dye solution while it was still hot, i.e. its temperature was ca. 80°C. After completion of the dye adsorption, the photoelectrode was withdrawn from the solution and washed thoroughly with ethanol to remove non-adsorbed dye under a stream of dry air or argon. A sandwich cell was prepared using the dye-sensitized electrode and platinum coated conducting glass electrode as the counter electrode. The latter was prepared by chemical deposition of platinum from 0·05 M hexachloroplatinic acid. The two electrodes were placed on top of each other using a thin poly-ethylene film (100 μm thick) as a spacer to form the electrolyte space. The empty cell was tightly held, and edges were heated to 130°C to seal the two electrodes together. The active surface area of the TiO_2 film electrode was ca. 0·74 cm^2. Three different liquid redox electrolytes and a polymer gel electrolyte were used in the test cells. They are AH1, AH2 and AH3. The composition of AH1 is 0·1 M I_2, 0·6 M 1,2-dimethyl-3-*n*-propylimidazolium iodide (DMPI) and 0·5 M *n*-methylbenzimidazolium iodide (NMBI) in γ-butyrolactone, AH2 is 0·5 M LiI, 0·05 M I_2 and 0·6 M tert-butyl pyridine (TBP) in acetonitrile and AH3 is 0·5 M DMPI, 0·5 M LiI and 0·05 M I_2 in

methoxy propionitrile (MPN). The electrolyte was introduced into the cell through a pre-drilled hole of the counter electrode, which was later closed by a cover glass to avoid the leakage of the electrolyte solution.

The polymer gel electrolyte was prepared following reported procedure with a slight modification.[22] The electrolyte composition was 1·4 g of polyacrylonitrile (PAN), 10 g of ethylene carbonate (EC), 5 ml of propylene carbonate (PC), 5 ml of acetonitrile, 1·5 g of LiI and 0·1 g of I_2. The gel electrolyte was cast onto the dye-coated TiO_2 film and pressed together with a platinum-coated FTO counter electrode under nitrogen atmosphere.

2.4 *Photoelectrochemical measurements*

The photovoltaic performance of the dye-sensitized nanocrystalline TiO_2 cells was determined using the simulator SOLARONIX SA SR-IV unit Type 312. The spectral response was determined by measuring the wavelength dependence of the incident photon-to-current conversion efficiency (IPCE) using light from a 100-W xenon lamp that was focused onto the cell through a double monochromator. The current-voltage characteristics were determined by applying an external potential bias to the cell and measuring the photocurrent using a Keithley model 2420 digital source meter and a 1000-W xenon lamp was used as the irradiation source. The spectral output of the lamp is set matched the AM 1·5 solar spectrum in the region of 350–750 nm (mismatch 1·9%).

3. Results and discussion

3.1 *Synthesis and characterization*

The photosensitizer [*meso*-Rhod-Zn-Rhod] was accomplished by adopting Knoevenagel condensation method. The triad was obtained in a quantitative yield and characterized by CHN analysis, MALDI-MS, IR, UV-Visible, ^{1}H NMR and fluorescence spectroscopies and cyclic voltammetry. MALDI-MS spectrum consists of molecular ion peak, which is ascribed to the presence of corresponding triad molecule. Figure 1 shows the absorption spectrum of triad was recorded in ethanol solvent and compared to that of triad adsorbed onto 6 μm thick nanocrystalline TiO_2 films. The absorption spectrum consists of an intense Soret band at 436 nm, assigned to a π–π^* transition to the second electronic

excited singlet state and two less intense Q-bands between 550 and 610 nm, corresponding to π–π^* transition to the first electronic excited singlet state. Both Soret and Q-bands are red shifted in comparison with its parent compound, i.e. ZnTPP. The red shift of absorption is probably due to the electron withdrawing nature of rhodanine moiety. This red shift was also observed in other rhodanine acetic acid substituted porphyrin dyads.[9] Both Soret and Q-bands of the triad are broadening when adsorbed onto nanocrystalline TiO_2 in comparison with its solution spectra (figure 1). The emission spectrum of triad was recorded at room temperature in dichloromethane solvent and the spectrum reveals characteristic vibronic bands of triad between 600 and
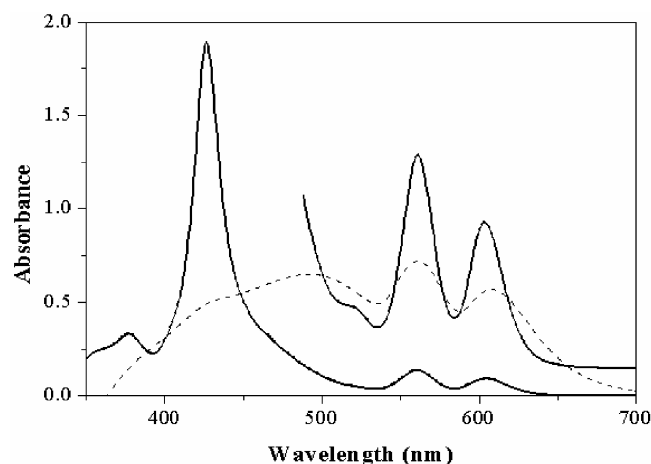
Figure 1. UV-Visible absorption spectra of [*meso*-Rhod-Zn-Rhod] (——) in ethanol, and (-------) adsorbed onto a TiO_2 film.
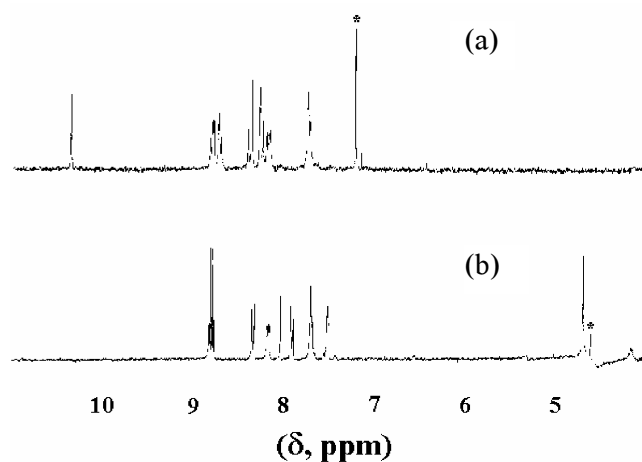
Figure 2. ^{1}H NMR spectra of (**a**) [CHO-Zn-CHO] in $CDCl_3$; (**b**) [*meso*-Rhod-Zn-Rhod] in DMSO-*d6*. The peak marked with an asterisk (*) is due to the solvent.

Table 1. Redox potential data of triad and reference compounds.[a]

| Compound | Potential (V vs SCE) | | |
	Oxidation[b]	Reduction[b]	E^*_{OX}/V
ZnTPP[c]	0·79	−1·40	−1·27
Rhodanine acetic acid[c]	1·58	−[e]	−
[*meso*-Zn-Rhod][c]	0·87	−0·96	−1·19
[*meso*-Rhod-Zn-Rhod][d]	0·70	−1·15	−1·34

[a]Error limits, $E_{1/2}$, ±0·03 V. [b]0·1 M TBAPF$_6$. [c]CH$_2$Cl$_2$. [d]Methanol. [e]No reduction was observed within solvent window. Excited state oxidation ponteital, $E^*_{OX} = E_{1/2} − E_{0-0}$[24]
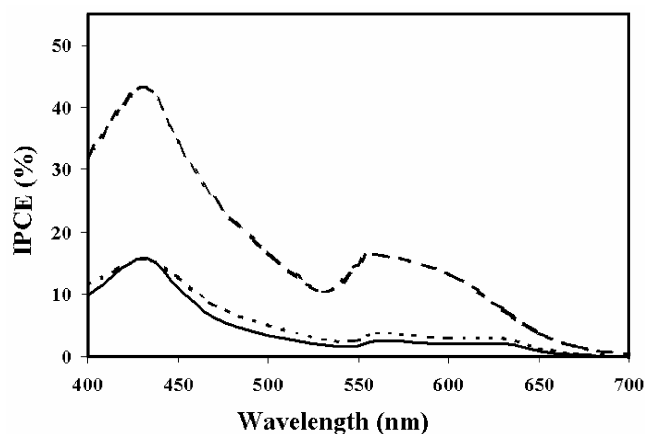
Figure 3. Photocurrent action spectra of [*meso*-Rhod-Zn-Rhod] sandwich-type cell using redox electrolytes AH1 (——), AH2 (······) and AH3 (------).

660 nm. The emission intensity was quenched in comparison with its individual constituent, i.e. ZnTPP. The quantum yield was obtained 0·014. No emission was observed for the porphyrin triad adsorbed onto 6 μm thick TiO$_2$ layer as a consequence of electron injection from excited singlet state of porphyrin into the conduction band of TiO$_2$.

The triad was further confirmed by ^{1}H NMR spectrum. Figure 2 shows the ^{1}H NMR spectra of triad [*meso*-Rhod-Zn-Rhod] and its individual constituent, i.e. [CHO-Zn-CHO]. In the *bis*-formyl porphyrin, the formyl peak appeared at 10·32 ppm where as in [*meso*-Rhod-Zn-Rhod] the formyl peak was absent indicating that the formyl group was reacted with rhodanine acetic acid group. The doublet at 7·55 ppm is belonging to the vinylic protons. The broad peak appeared at 4·80 ppm corresponds to N-CH$_2$ protons of rhodanine acetic acid group. The absence of formyl proton signal and presence of vinylic proton signal in [*meso*-Rhod-Zn-Rhod] indicates the formation of the compound.

With a view to evaluate HOMO-LUMO levels of new photosensitizer, we have carried out the elec-

trochemical investigations. For solubility reason, the redox potentials of the triad [*meso*-Rhod-Zn-Rhod] were performed in methanol where as its individual constituents, i.e. ZnTPP and rhodanine acetic acid were measured in dichloromethane solvent. The redox potentials were measured by both cyclic and differential pulse voltammetric techniques. The redox potentials of triad, dyad and its individual constituents were presented in table 1. From the table, it is clear that the triad undergoes one oxidation and one reduction at 0·70 and −1·15 V, respectively, within the solvent window. Where as its dyad has oxidation at 0·87 V and reduction at −0·96 V.

3.2 *Photovoltaic measurements*

The performance of the new sensitizer has been studied in a regenerative photo-electrochemical cell using three different liquid redox electrolytes as well as a polymer gel electrolyte, a quasi-solid-state DSSC. The test cell results are compared with [*meso*-Zn-Rhod] both in liquid and polymer gel electrolyte. The photocurrent action spectra of [*meso*-Rhod-Zn-Rhod] in all three liquid redox electrolytes were shown in figure 3, where the incident monochromatic photon-to-current conversion efficiencies (IPCE) values are plotted as a function of the excitation wavelength. The IPCE (λ) is defined by the (1)

$$IPCE(\lambda) = 12\,400\,(J_{SC}/\lambda\phi), \qquad (1)$$

where λ is the wavelength (nm), J_{SC} is the photocurrent density under short-circuit conditions (mA/cm^2) and ϕ is the incident radiative flux (mW/cm^2). As expected the shape of action spectrum clearly follows the shape of the absorption spectrum in solution and that of the porphyrin adsorbed on TiO$_2$. We have observed the IPCE of 43% at Soret band and 20% at Q-bands of [*meso*-Rhod-Zn-Rhod] in AH3

Table 2. Comparison of short-circuit photocurrent density (J_{SC}), open-circuit photovoltage (V_{OC}), fill factor (*ff*) and overall conversion efficiency (η) for the DSSC using new photosensitizer along with [*meso*-Zn-Rhod] in redox electrolyte 0·5 M DMPI, 0·5 M LiI and 0·05 M I_2 in methoxy propionitrile (AH3) and polymer gel redox electrolyte.

Sensitizer	Redox electrolyte	J_{SC} (mA/cm^2)[a]	V_{OC} (mV)[a]	*ff*(%)[a]	η (%)
[*meso*-Rhod-Zn-Rhod]	AH1	1·14	590	0·71	0·47
[*meso*-Rhod-Zn-Rhod]	AH2	0·91	540	0·65	0·32
[*meso*-Rhod-Zn-Rhod]	AH3	3·51	400	0·55	0·76
[*meso*-Zn-Rhod]	AH3	2·79	397	0·50	0·55
[*meso*-Rhod-Zn-Rhod]	Polymer gel	1·52	373	0·48	0·27
[*meso*-Zn-Rhod]	Polymer gel	1·64	476	0·49	0·38

[a]Error limits, J_{SC}, ± 0·1 mA/cm^2; V_{OC}, ± 30 mV and *ff*, ± 0·03
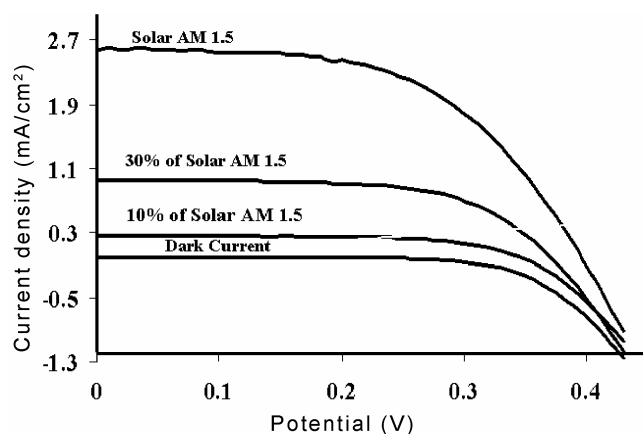
Figure 4. Photocurrent-voltage characteristics of a nanocrystalline photovoltaic cell sensitized with triad [*meso*-Rhod-Zn-Rhod], using redox electrolyte 0·5 M DMPI, 0·5 M LiI and 0·05 M I_2 in MPN (AH3).

Figure 5. Photocurrent action spectra of [*meso*-Rhod-Zn-Rhod] (-------), and [*meso*-Zn-Rhod] (———) sandwich-type cell using a polymer gel redox electrolyte.

redox electrolyte. Under similar conditions, the IPCE of [*meso*-Zn-Rhod] was observed to be 34 and 11% at Soret and Q-bands, respectively. This may be due to the presence of two anchoring rhodanine acetic acid groups at *meso*-positions of [*meso*-Rhod-Zn-Rhod], which strongly bind and efficiently inject the excited electron from sensitizer to the TiO_2 conduction band. Figure 4 shows the photocurrent-voltage characteristics obtained with a DSSC under illumination of simulated solar light. The I–V curves in figure 4 refer to the [*meso*-Rhod-Zn-Rhod] dye-coated TiO_2 films under 100, 30, 10 and 0% of AM 1·5 irradiation and the data are presented in table 2 for all the three liquid redox electrolytes along with [*meso*-Zn-Rhod].

The overall conversion efficiency (η) of the photovoltaic cell is calculated from the integrated photocurrent density (J_{SC}), the open-circuit photovoltage (V_{OC}), the fill factor of the cell (*ff*) and the intensity of the incident light (I_{ph}).

$$\eta = J_{SC} V_{OC} ff/I_{ph}. \qquad (2)$$

The fill factor is defined by the following equation.

$$ff = \frac{J_{PH(\max)} X V_{PH(\max)}}{J_{SC} X V_{OC}}, \qquad 3)$$

where $J_{PH(\max)}$ and $V_{PH(\max)}$ are the photocurrent and photovoltage for maximum power output and J_{SC} and V_{OC} are the short-circuit photocurrent density and open-circuit photovoltage. From the table 2, it is clear that the maximum efficiency obtained was 0·76% in AH3 redox electrolyte. The value is high when compared with [*meso*-Zn-Rhod]. This may be due to the presence of two anchoring groups in [*meso*-Rhod-Zn-Rhod] which adsorb and efficiently inject excited electrons into TiO_2 conduction band than in [*meso*-Zn-Rhod].

For the estimation of durability of DSSC, we have also performed test cell studies by using a polymer

gel electrolyte, a quasi-solid-state DSSC of both [*meso*-Zn-Rhod] and [*meso*-Rhod-Zn-Rhod]. The photocurrent action spectra of both dyes in polymer gel electrolyte were presented in figure 5 showed the IPCE 12·5 and 16% at 430 nm i.e. Soret band and 3·5 and 6% at 550 nm i.e. Q-bands of [*meso*-Zn-Rhod] and [*meso*-Rhod-Zn-Rhod], respectively. Figure 6 shows the photocurrent-voltage characteristics obtained with a DSSC under illumination of simulated solar light. The efficiency was found to be 0·38 and 0·29% for [*meso*-Zn-Rhod] and [*meso*-Rhod-Zn-Rhod], respectively.

The η term is essentially controlled by two parameters: (i) the rate of electron transfer by the iodide oxidation to the oxidized porphyrin after electron injection (k_{reg}) and (ii) the rate of charge recombination of the oxidized porphyrin with conduction band electrons (k_{CR}), as shown in energy level scheme (figure 7). k_{reg} can not be considered as a limiting factor because the ground-state oxidation potentials of the both dyad and triad are positive than those of the best dyes that yield very high IPCE's.[23] Considering the redox potentials of the I^-/I_3^- redox couple (0·2 V vs SCE),[25] the free-energy of the latter electron transfer reaction is energetically more favourable for dyad ($\Delta G = -0.90$ eV) than the triad ($\Delta G = -0.69$). Unlike in ruthenium polypyridyl complexes, the charge recombination process between negative charge (electrons in TiO_2) and the positive charge (oxidized porphyrin) sensitizers are faster. However, Durrant *et al* have reported that the rate of charge recombination between conduction band electrons and oxidized porphyrin sensitizers is
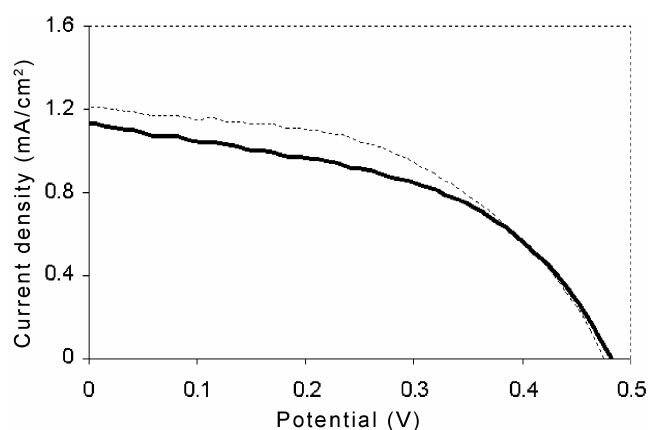
in the range of several milliseconds.[26] This rate is sufficiently slow to permit the regeneration of the ground state of the porphyrin by the iodide in solution. The other factors, which influence the IPCE, are the electron-injection quantum yield (ϕ_{inj}), which directly depends on the electron-injection rate (k_{inj}). Both ϕ_{inj} and k_{inj} are probably high in triad than in dyad as evidenced by high IPCE of triad, which has two anchoring groups in liquid redox electrolyte. This in turn reflects in J_{SC} as well as efficiency of DSSC.

While using polymer gel redox electrolyte, the η is found less in comparison with liquid redox electrolyte. This may be probably due to the charge carriers that are not able to contribute to the conduction process being manifested in terms of low current density even though the IPCE is reasonably good. The reason for this may be because of the internal resistance of the cell. The internal resistance of the cell comprises of resistance of the conducting glass, electron transfer rate at FTO/TiO_2, TiO_2/TiO_2, Pt/electrolyte and TiO_2/electrolyte interfaces. Of these, TiO_2/electrolyte interface is significant in the case of polymer gel electrolyte, as the electrolyte
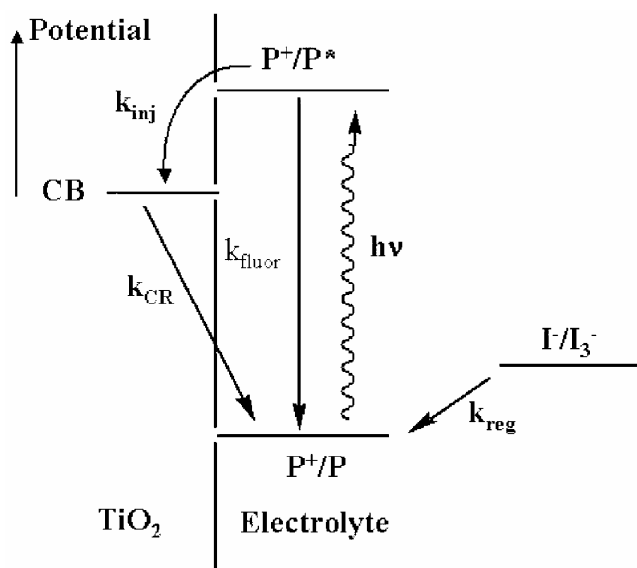
Figure 7. Schematic representation of the different reactions occurring at the TiO_2 photoelectrode surface: CB is the conduction band, k_{fluor} is the rate constant of the fluorescence deactivation of the porphyrin excited state, k_{inj} is the rate constant of the photoinduced electron transfer from porphyrin excited state, k_{CR} is the rate constant of the charge recombination between the oxidized porphyrin and electrons in the CB, k_{reg} is the rate constant of the electron-transfer reaction between the oxidized porphyrin and the iodide in the electrolyte.

Figure 6. Photcurrent-voltage characteristics of a nanocrystalline photovoltaic cell sensitized with triad [*meso*-Rhod-Zn-Rhod] (———) and [*meso*-Zn-Rhod] (-----) using a polymer gel redox electrolyte.

would not efficiently penetrate into TiO_2 pores as in the case of liquid electrolyte. As a result air is being locked in the unfilled area affecting the photocurrent of DSSC.[22,27] We have observed the efficiencies of dyad and triad to be 0·38 and 0·29%, respectively which is relatively low as compared to AH3 liquid redox electrolyte where the IPCE of triad is higher than dyad. In this case also it may be again due to the internal resistance of the cell as explained above and it is evidenced in short-circuit current densities.

4. Conclusions

In conclusion, we have synthesized a triad, [*meso*-Rhod-Zn-Rhod] having two rhodanine acetic acid groups *trans* to each other and characterized by UV-Vis, ^{1}H NMR, MALDI-MS, CHN analysis and cyclic voltammetry. The new sensitizer was tested in DSSC by using three different liquid redox electrolytes and compared with dyad. In order to overcome the liquid redox electrolyte problems, both dyad and triad were tested in DSSC by using polymer gel electrolyte (quasi-solid-state DSSC). The DSSC with polymer gel electrolyte is found to be more durable than liquid redox electrolyte.

Acknowledgements

References

1. O'Regan B and Gratzel M 1991 *Nature* **353** 737
2. Gratzel M 2001 *Nature* **414** 338
3. Gratzel M 2006 *Curr. Appl. Phys.* **6S1** e2
4. Durrant J R, Haque S A and Palomares E 2006 *Chem. Commun.* 3279
5. Gratzel M 2000 *Prog. Photovolt. Res. Appl.* **8** 171
6. Craig R R, Ward M D, Nazeeruddin M K and Gratzel M 2000 *New J. Chem.* **24** 651
7. Shklover V, Spiccia L, Deacon G B, Bignozzi C A and Gratzel M 2001 *J. Am. Chem. Soc.* **123** 1613
8. Giribabu L, Chandrasekharam M, Lakshmi Kantam M, Reddy V G, Satyanarayana D, Rao O S and Reddy P Y 2006 *Indian J. Chem.* **Sec. A45** 629
9. Giribabu L, Vijaykumar Ch and Reddy P Y 2006 *J. Porphyrins and Phthalocyanines* **10** 1007
10. Reddy P Y, Giribabu L, Lyness C, Snaith H J, Vijaykumar Ch, Chandrasekharam M, Lakshmi Kantam M, Yum J-H, Kalyanasundaram K, Gratzel M and Nazeeruddin M K 2007 *Angew. Chem. Int. Ed* **46** 373
11. Giribabu L, Ch. Vijaykumar, Reddy V G, Reddy P Y, Rao Ch S, Jang S R, Yum J H, Gratzel M and Nazeeruddin M K 2007 *Solar Energy Materials and Solar Cells* **91** 1611
12. Wasmer C C, Kim H S and Lee J K 2002 *Opt. Mater.* **21** 221
13. Odobel F, Blart E, Lagree M, Villieras M, Boujtita H, Murr N E, Caramori S and Bignozzi C A 2003 *J. Mater. Chem.* **13** 502
14. Jasieniak J, Jhonston M and Waclawik E R 2004 *J. Phys. Chem.* **B108** 12962
15. Campbell W M, Burrell A K, Officer D L and Jolley K W 2004 *Coord. Chem. Rev.* **248** 1363
16. Wang Q, Campbell W M, Bonfantani E E, Jolley K W, Officer D L, Walsh P J, Gordon K, Humphry-Baker R, Nazeeruddin M K and Gratzel M 2005 *J. Phys. Chem.* **B109** 15397
17. Perrin D D, Armarego W L F and Perrin D R 1980 *Purification of laboratory chemicals* (Oxford)
18. Pomogailo A D, Razumov V F and Voloshanovskii I S 2000 *J. Porphyrins and Phthalocyanines* **4** 45
19. Harimmon A and Davila J 1989 *Tetrahedron* **45** 4737
20. Wang P, Zakeeruddin S M, Comte P, Charvet R, Humphry-Baker R and Gratzel M 1996 *J. Phys. Chem.* **100** 16502
21. Barbe C J, Arendse F, Comte P, Jirousek M, Lenzmann F, Shklover V and Gratzel M 1987 *J. Am. Chem. Soc.* **80** 3157
22. Cao F, Oskam G and Searson P C 1995 *J. Phys. Chem.* **99** 17071
23. Kalyanasundrm K and Gratzel M 1998 *Coord. Chem. Rev.* **77** 347
24. E_{0-0} values of ZnTPP, dyad and triad are 2·06, 2·06 and 2·04 eV ($\pm 0·05$), respectively
25. Hagfeldt A and Gratzel M 1995 *Chem. Rev.* **95** 49
26. Clifford J N, Yahioglu G, Milgrom L R and Durrant J R 2002 *Chem. Commun.* 1230
27. Hoshikawa T, Yamada M, Kikuchi R and Eguchi K 2005 *J. Electrochem. Soc.* **152** E68